DOI: 10.61782/fa.2023.0833

forum acusticum 2023

A DATASET FOR LOCATION- AND DIRECTION-DEPENDENT REVERBERATION ANALYSIS

Benoit Alary[1*] **Archontis Politis**[2]
[1] STMS, IRCAM, Sorbonne Université, CNRS, Ministère de la Culture, Paris, France
[2] Audio Research Group, Computing Sciences Unit, Tampere University, Tampere, Finland

ABSTRACT

Measuring room impulse responses (RIRs) is fundamental to sound reproduction and acoustical research. For instance, these measurements play an essential role in building digital twins in virtual reality to preserve their cultural heritage. For sound reproduction, RIRs can be used directly through convolution, or a more complex time-frequency domain analysis may be used to characterize a parametric method. Measuring RIRs using microphone arrays, such as a spherical microphone array, is necessary to extend this reproduction to the spatial domain. Recent work has shown that reverberant sound fields have perceptually salient position- and direction-dependent characteristics which should be considered in six degrees of freedom (6DoF) sound reproduction. However, related psychoacoustics and signal processing research require complex datasets to measure to better understand these characteristics. In this article, we present an experiment carried out in the main auditorium of the Finnish National Opera and Ballet in Helsinki, where we measured spatial RIRs from the perspective of ninety-seven individual seats. We analyze key characteristics of the resulting anisotropic and inhomogeneous sound field using energy-based analysis methods and the dataset is shared publicly to allow for further research in this field, such as multi-slope decay analysis and 6DoF auralization.

Keywords: *Anisotropy, inhomogeneity, auralization, directional reverberation, virtual reality.*

**Corresponding author*: *Benoit.Alary@ircam.fr.*

1. INTRODUCTION

A measured room impulse response (RIR) contains information on the time-frequency behavior of sound waves in a room for a set of specific measurement conditions, such as a microphone and loudspeaker position. As such, an RIR may be used to detect the incident direction of early reflections [1], to study specific acoustics characteristics such as variable acoustics room [2, 3] or coupled volume [4], and analyze properties of a late reverberant sound field [5, 6, 7]. Larger datasets of measured RIRs [8] find applications in speech recognition [9], conservation of acoustics [10, 11], machine learning [12, 13], and studying the perception of transitioning through coupled rooms [14].

In virtual and augmented reality (VR/AR) applications, where reproduction accuracy and six degrees of freedom (6DoF) scene navigation are important, new challenges arise for acoustic reproduction [15, 16, 17, 18, 19]. For sound field reproduction, a spherical microphone array (SMA) is typically used to measure spatial room impulse responses (SRIR), which can be used for reproduction using convolution [20], or spatial-time-frequency processing may be used to improve efficiency and accuracy of the reproduction [21, 19].

While reverberation is often described as diffused in time, recent acoustics measurement research has demonstrated that reverberant sound fields are not necessarily isotropic [22, 23, 6, 24], and may have perceptually salient position- and direction-dependent decay characteristics [25], which should also be considered in 6dof auralization [26]. However, since the perceptual effect of anisotropic reverberation will vary from one room to another and the perceptual threshold of such characteristics has not yet been fully established, more research is required to fully understand this aspect.

In the study of anisotropic and inhomogeneous sound fields, opera houses offer interesting characteristics. Indeed, while they are built to encourage a certain amount

of reverberation in the audience section, they also contain large open spaces behind the stage as well as an orchestral pit and high ceilings, which all contributes to a non-uniform spatial distribution of sound energy throughout the decay. A previous experiment was performed in an opera hall to capture SRIRs from fifteen seats [26] and propose the use of a directional feedback delay network reverberator for reproduction [27, 28]. However, a relatively large inhomogeneity was observed between adjacent measurement points, suggesting the necessity to reduce the distances between each measurement point.

In this article, we present an extended measurement campaign carried out in the main auditorium of the Finnish National Opera and Ballet in Helsinki, where SRIRs were measured from the perspective of ninety-seven individual seats in the parterre section. Using energy-based analysis methods, we analyze the sound field to confirm it contains both anisotropic and inhomogeneous characteristics. The dataset is shared publicly to allow its use in future research, including directional and multi-slope decay analysis, and 6DoF auralization. Since the stage curtain was raised during measurement, and the stage was left empty, the measurement conditions are not ideal for assessing the acoustics qualities of this opera hall, in a musical sense. Nonetheless, the dataset aims to offer an interesting set of sound field characteristics and challenges for future research in reverberation modeling and reproduction. The dataset, titled OperaRIR, is available publically at `https://doi.org/10.5281/zenodo.8096639`.

2. DATASET

2.1 Description

The main auditorium of the Finnish National Opera and Ballet (FNOB), located in Helsinki, Finland, is a modern-shaped horseshoe opera hall that opened in 1993. The hall contains three balconies and a parterre, for a total of 1350 seats. The parterre contains 731 individual seats over 19 rows. In its widest section, the hall is approximately 27 m wide, and 25 m deep, from the center back of the hall to the beginning of the stage, including the orchestra pit.

In this measurement campaign, 210 SRIRs were measured. More specifically, 97 individual seats located on the parterre were measured sequentially using two different sound sources located on the stage (Fig.1), for a total of 194 SRIRS. Among these measurement positions, four were selected as validation points, and two extra measurement sets were performed, using the same two sound sources, thus adding 16 SRIRs to the dataset. These validation points are intended for use in assessing the stability of the measurements and the background noise.

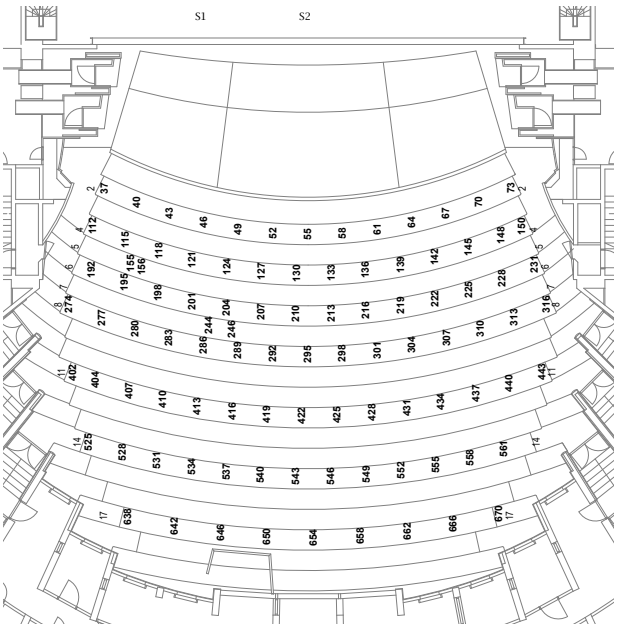

Figure 1. Measurement layout.

The measurements were captured using an SMA, the Eigenmike® [1] , to obtain microphone signals that can be encoded as fourth-order ambisonic SRIRs. Two Genelec 8331A loudspeakers were used as sound sources and both were positioned at a depth of one meter, from the edge of the stage, on a 1.6 m stand. The first source was located 5.53 m from the lateral center, on the left side of the stage when looking from the parterre, and the second loudspeaker was located in the center 1. Other than the loudspeakers, the stage was left completely empty, the curtain was fully raised, and no audience was present. Therefore, in practice, the perceived reverberant sound field would be different during a live performance.

While the use of an omnidirectional sound source, such as a dodecahedron, is recommended to measure acoustic parameters and measurements [29], we observed during the first experiment ([26]) that the deviation of omnidirectionality was unpredictable at mid-high frequencies, and that the loss of phase coherence due to their multi-driver operation was resulting in measurements that

[1] https://mhacoustics.com/

Table 1. Microphone coordinates of the first two measured rows contained in the dataset.

row	seat	x	y	row	seat	x	y
2	37	3.51	7.80	4	112	3.00	9.56
	40	4.97	8.35		115	4.47	10.17
	43	6.52	8.87		118	5.97	10.71
	46	8.06	9.29		121	7.54	11.15
	49	9.60	9.58		124	9.12	11.44
	52	11.19	9.79		127	10.68	11.66
	55	12.81	9.86		130	12.28	11.72
	58	14.44	9.79		133	13.89	11.69
	61	16.02	9.60		136	15.48	11.59
	64	17.58	9.32		139	17.04	11.35
	67	19.14	8.91		142	18.62	11.03
	70	20.64	8.37		145	20.16	10.58
	73	22.11	7.72		148	21.69	10.01
					150	22.62	9.56

were sub-optimal for analysis and sound reproduction. Hence a high-quality, two-way studio monitor, was preferred as the excitation source, and its directivity is considered a property of the measurements.

The SRIRs were measured using 30-second long exponential sine sweeps [30, 31]. The loudness of each loudspeaker was adjusted using a sound pressure level (SPL) meter from an arbitrary position in the far field. However, after detecting some clipping in the output of the first source at high frequencies, the frequency range of the sweep used was restricted as a precaution. More specifically, we used a sweep covering a frequency range of 50 Hz to 16 kHz for the first sound source, and a sweep covering a frequency range 50 Hz to to 20 kHz for the second source. Nonetheless, spatial analysis in the 16 kHz-20 kHz frequency range are never recommended when using such an SMA due to physical limitations.

The locations of the measurement points were chosen to cover as much of the parterre given time constraints in the availability of the hall for measurements. For the first half of the parterre, closer to the stage, every second row was measured, and in the second half of the hall, every third row. For most measured rows, two non-measured seats were left between each measured one, and this was extended to four seats on the last row. The average lateral distance between two measured seats in the same row was 1.57 m, and the average depth distance between two measured rows was 1.58 m. Throughout the measurement campaign, the microphone was placed on the floor directly in front of a seat, using a 1.4 m tall stand. The location of each microphone position was obtained using a top-view architectural plan of the hall (Fig.1). The coordinate system used here is in meters and the axis origin is located in the top left corner of the architectural plan, the two loudspeakers are positioned at $y = 0$. As such, the coordinates of the first source are $(7.30, 0.0)$, and the second source is located at $(12.83, 0.0)$.

In post-processing, the overall maximum amplitude value detected across the whole dataset was used to normalize the dataset while preserving the relative differences between measurements. The public dataset contains the deconvolved impulse responses, both as 32-channel microphone signals, as well as fourth-order Ambisonic files encoded with the ACN channel ordering and SN3D normalization. The SRIRs were measured at 48 hKz. The coordinates of each measurement position are provided in a separate data file (Table 1).

2.2 Alignment

One significant challenge of measuring a hall from many positions is ensuring a consistent alignment of the microphone for each measurement position. Since this hall contains no parallel walls to align with, and each seat has a slightly different rotation angle on the parterre, the front of the spherical microphone was aligned horizontally using a laser pointer, aiming at the loudspeaker located in the center of the stage. Therefore, each measurement of the dataset uses a different alignment which needs to be compensated during post-processing.

In the dataset's coordinate system, the alignment reference point is located at $(12.83, 0)$. The exact orientation angle was obtained by a combination of geometrical prior knowledge and acoustical evidence from the measured SRIRs. More specifically, for each position a windowed SRIR was obtained by applying a rectangular window around the maximum peak of the omnidirectional RIR to all channels, hence isolating the direct path component. This windowed SRIR was then analyzed to detect the direction-of-arrival (DOA) of the direct path, using a plane wave decomposition approach, band-limited between 2–6 kHz, followed by peak finding on the plane wave amplitude distribution. The azimuth component of the obtained DOA combined with the azimuth of the line connecting the measurement position and the source was then used to obtain the azimuthal rotation of the Eigenmike in the global coordinate system. Based on the analyzed azimuthal rotation angle for each measurement position, the Ambisonic recordings were inversely rotated to

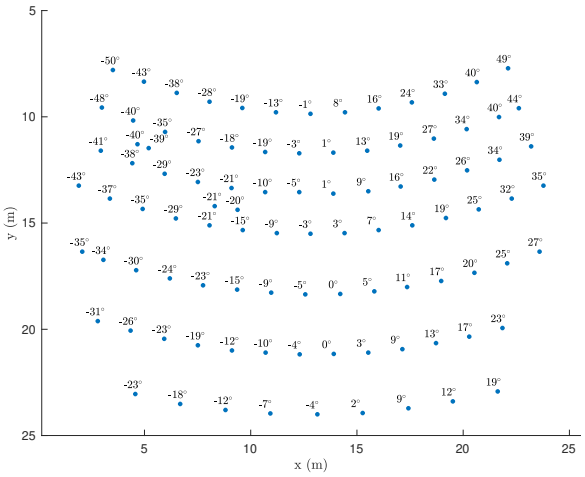

Figure 2. Lateral rotation angle of the SMA used during measurements.

face the back wall of the stage (Fig.2). Compensation angles, original measured files, and rotated HOA files are all provided in the dataset.

2.3 Control points

In the context of sound reproduction, determining the optimal distance between measurement points remains an open question. In order to assess the homogeneity of the sound field at shorter distances, two pairs of seats were measured with a shorter distance between them. The first pair, measured on row 5, has a distance of 0.28 m between the two microphone positions, and the second pair, on row 7, has a distance of 0.55 m. These measurement points lie outside the main grid points used for the rest of the measurement campaign and may be of interest in the study of 6dof interpolation. These two pairs of seats were measured three times consecutively to study the stability of the measurement method.

3. ENERGY-DECAY ANALYSIS

In the context of sound reproduction, a common analysis approach for reverberant sound fields is to analyze the decay of energy over time [32]. While energy-decay analysis has some drawbacks, such as sensitivity to environmental noise, it provides useful measures in the context of artificial reverberation as they correspond well to our perception of sound decay. Additionally, time-frequency analysis of late reverberation in a measured RIR may be performed using a filter bank [33]. For SRIRs, this analysis is extended to a set of angles to obtain direction-dependent characteristics [25]. As such, directional room impulse responses (DRIRs) are obtained from a measured SRIR encoded in spherical harmonics (SHs) using plane wave decomposition for a set of angles distributed around the sphere

$$y(n, \phi, \theta) = \mathbf{y}^T(\phi, \theta)\, \mathbf{s}(n), \tag{1}$$

where $\mathbf{s}(n) = [s_1(n), ..., s_{(L+1)^2}(n)]^T$ is the L-th order ambisonic SRIR, and $\mathbf{y} = [Y_{0,0}, Y_{1,-1} ..., Y_{L,L}]^T$ is a vector of SH values for a pair of azimuth and elevation angles (ϕ, θ). Directional, and frequency-dependent, decay curves are calculated from a DRIR using [6, 25]

$$\mathrm{EDC}(n, \omega, \phi, \theta) = 10\, \log_{10} \left(\sum_{i=n}^{N} \left(y(i, \omega, \phi, \theta) \right)^2 \right), \tag{2}$$

where ω is the center frequency of a band in a filter bank. As such, energy-decay analysis can be performed for different time segments (n), frequencies (ω), and directions (ϕ, θ). When visualizing results, we limit some of these parameters to allow comparison of specific time-frequency-directional aspects.

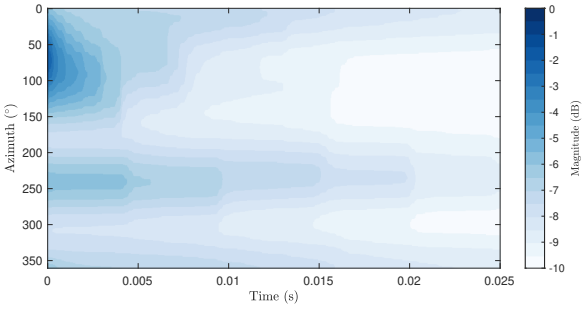

Figure 3. Directional EDC results on the horizontal plane, for the first 25 ms of an SRIR filtered between 1 kHz and 3 kHz, measured in front of seat 37, on the second row, using the first sound source.

3.1 Energy-decay on the horizontal plane

Using the SRIR measured on seat 37, on the second row, and the first sound source, located on the left of the stage, the response was filtered using a bandpass between 1 kHz and 3 kHz. In Fig.3-5, an energy-decay analysis is performed on a set of azimuthal angles around the sphere, for a fixed elevation angle (0°). On the analyzed plane,

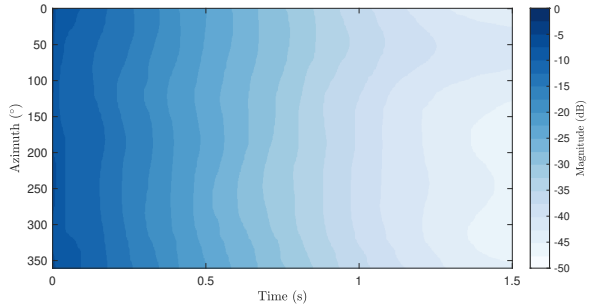

Figure 4. Directional EDC results on the horizontal plane, for the first 1.5 seconds of an SRIR filtered between 1 kHz and 3 kHz, measured in front of seat 37, on the second row, using the first sound source.

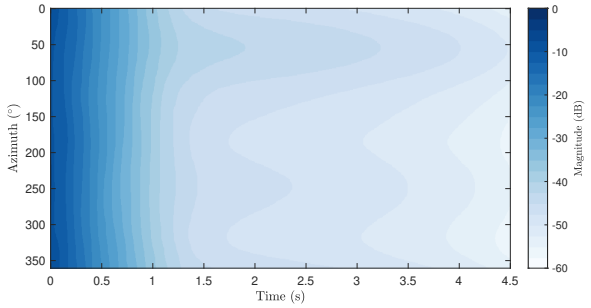

Figure 5. Directional EDC results on the horizontal plane, for the first 4.5 seconds of an SRIR filtered between 1 kHz and 3 kHz, measured in front of seat 37, on the second row, using the first sound source.

from the perspective of an audience member looking towards the stage, an azimuth angle 0° is to the right, 90° is towards the stage, 180° is to the left, and 270° is behind.

For any given time step, the directional decay analysis contains the sum of the remaining decay energy in that direction (Fig.2). Figure 3 contains results for the first 25 ms of the measured SRIR. We observe that the direct sound is incident to 75°, thus slightly to the right from the perspective of the parterre. We also observe that the decay energy is slightly stronger at 0° and 235°in the first 25ms of decay.

In Fig.4, which contains analysis results for the first 1.5 seconds, more energy is centered around 335° in the first 100 ms, before gradually migrating to 15° and 175° at around 0.5 seconds. In any SRIR measurements, some background noise will inevitably occur and the energy needs to be taken into consideration when interpreting decay analysis. In the later part of the measured sound field, the background noise is noticeably present towards 60° and 250° (Fig.5), which appears to interfere with the analysis results already at 1 second. For sound reproduction, it is highly recommended to use denoising methods to avoid an unnatural reverberation effect when convolving with this noise [34].

3.2 Energy-decay deviation

In a homogeneous sound field, sound energy is uniformly distributed to any point in space, and in an isotropic sound field, the energy incident to a point is uniformly distributed from any direction. In practice, these theoretical requirements for a diffuse sound field are never fully realized and it becomes interesting to quantify how much we deviate from this uniformity energy principle. The energy-decay deviation (EDD) [6, 25], is a measure of the deviation between direction-dependent $\mathrm{EDC}(n, \phi, \theta)$ to a mean

$$\mathrm{EDD}(n, \phi, \theta) = \mathrm{EDC}(n, \phi, \theta) - \overline{\mathrm{EDC}}(n). \qquad (3)$$

where $\overline{\mathrm{EDC}}(n)$ corresponds to the omnidirectional and location-independent mean.

For the purpose of this dataset, we are interested in the study of both anisotropy and inhomogeneity and as such, the $\overline{\mathrm{EDC}}(n)$ is calculated from a set of directions distributed on the top hemisphere, for every measurement point. Using this approach, we can analyze how the energy is distributed in the measured area, at different times. At time zero, time-aligned from the initial impulse for each seat, in Fig.6, the location of the first sound source can clearly be identified as coming from the front left of the stage, represented in the top-left corner of the figure, while the overall reverberant energy decreases as the measuring point gets further away from the source.

In Fig.7, we can observe that at 1 second, more reverberant energy between 3kHz and 5kHz originates from the ceiling compared to the first two and last measured rows. This may be explained by the presence of a different ceiling material directly above the first two measured rows.

In Fig.8, representing the EDD of the reverberant sound field at six seconds, we observe the most prominent energy, which is caused by noise at this point in time, originates from the stage area. This energy is slightly less prominent in seats located on the right side of the parterre, suggesting that the source of the noise was either directional or obstructed in some way.

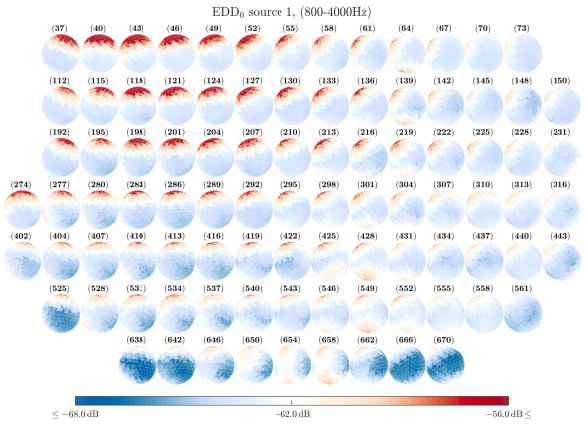

Figure 6. Top view analysis of each measured rows, at time 0 seconds.

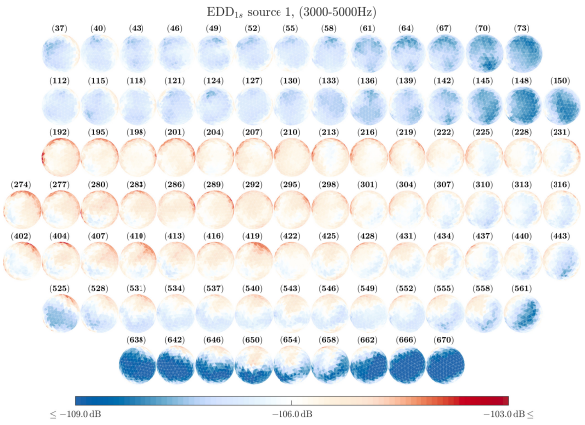

Figure 7. Top view analysis of each measured rows, at time 1 second.

3.3 Reverberation Time

An important characteristic of a reverberant sound field is the reverberation time, T_{60}. Here again, for spatial analysis, we favor a directional analysis from a set of DRIRs ($T_{60}(\phi, \theta)$). The decay analysis time window used here starts after the mixing time and before the noise floor is reached [34]. The mixing time is established using a spatial incoherence evaluation method to find the transition point between early and late reverberation ([35, 34]). In Fig.9, we can observe the $T_{60}(\phi, \theta)$ of the middle seats in two different rows, 2 and 6. The shorter reverberation time coming from above seat 55 and longer $T_{60}(\phi, \theta)$ above

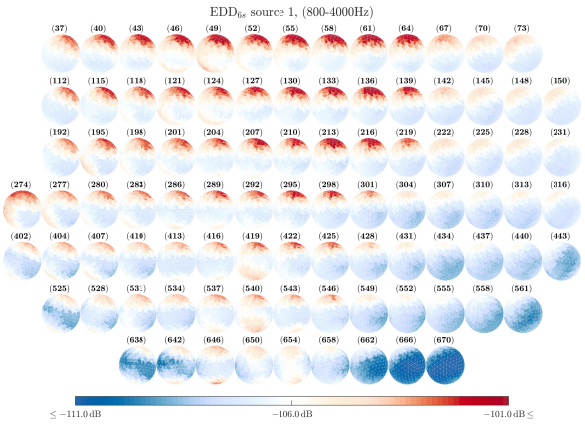

Figure 8. Top view analysis of each measured rows, at time 6 seconds.

seat 210 are consistent with what is observed in Fig.7.

Overall, through these energy-based analyses, we observe that the sound field should be considered both anisotropic and inhomogeneous. Further analysis also shows that the energy distribution during the early part of the reverberation is not a predictor of the behavior during late reverberation, which suggests that its reproduction would require direction-dependent decay characteristics.

4. CONCLUSION

This article introduced a dataset of measured SRIRs in the opera house of the FNOB located in Helsinki, Finland. Two directional sound sources were used on the stage along with 97 microphone positions distributed in the parterre section. A 32-channel SMA was used producing fourth-order Ambisonics SRIRs that allow further spatial analysis. Energy-based analysis methods confirmed that the reverberant sound field of the parterre area is non-uniform. This dataset is shared publicly and intended to help advance research on anisotropic and inhomogeneous reverberant field modeling and reproduction methods.

5. ACKNOWLEDGMENTS

The measurement campaign was part of a postdoctoral project funded by the Kaute Foundation (project ”Conservation of the Acoustics of Historical Halls in Helsinki”). The authors would like to thank Jaakko Korkalainen and Timo Tuovila, from the Finnish National Opera and Ballet, for their help and invaluable support.

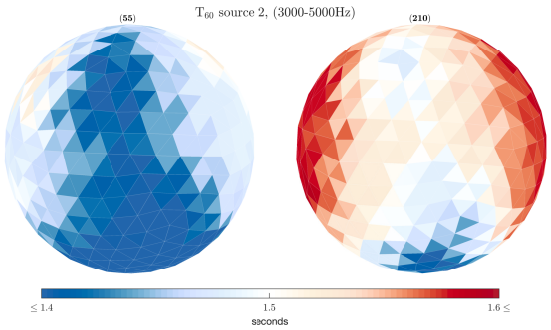

Figure 9. $T_{60}(\phi, \theta)$ analysis of the top hemisphere of two middle seats, located respectively on rows 2 and 6.

6. REFERENCES

[1] R. Stewart and M. B. Sandler, "Statistical measures of early reflections of room impulse responses," in *Proc. Int. Conf. on Digital Audio Effects (DAFx)*, (Bordeaux, France), Sept. 2007.

[2] K. Prawda, S. J. Schlecht, and V. Välimäki, "Calibrating the Sabine and Eyring formulas," *The Journal of the Acoustical Society of America*, vol. 152, pp. 1158–1169, Aug. 2022.

[3] F. Klein and S. V. Amengual Garí, "The r3vival dataset: Repository of room responses and 360 videos of a variable acoustics lab," in *ICASSP 2023 - 2023 IEEE International Conference on Acoustics, Speech and Signal Processing (ICASSP)*, pp. 1–5, 2023.

[4] P. Luizard and B. F. G. Katz, "Coupled volume multi-slope room impulse responses: a quantitative analysis method," in *Proceedings of the 8th International Conference on Auditorium Acoustics*, (Dublin, Ireland), pp. 169–176, 2011.

[5] B. N. Gover, J. G. Ryan, and M. R. Stinson, "Measurements of directional properties of reverberant sound fields in rooms using a spherical microphone array," *J. Acoust. Soc. Am.*, vol. 116, pp. 2138–2148, Oct. 2004.

[6] B. Alary, P. Massé, V. Välimäki, and M. Noisternig, "Assessing the anisotropic features of spatial impulse responses," in *Proc. EAA Spatial Audio Signal Processing Symposium*, (Paris, France), pp. 43–48, Sep. 2019.

[7] C. Hold, T. Mckenzie, G. Götz, S. J. Schlecht, and V. Pulkki, "Resynthesis of spatial room impulse response tails with anisotropic multi-slope decays," *journal of the audio engineering society*, vol. 70, pp. 526–538, june 2022.

[8] T. Piquet, H. Teyssier, E. Ouellet-Delorme, R. Duée, and N. Bouillot, "Two datasets of room impulse responses for navigation in 6 degrees of freedom: a symphonic concert hall and a former planetarium," in *25th International Conference on Digital Audio Effects DAFx20*, (Vienna University of Music and Performing Arts (mdw), Austria), pp. 169–176, sep 2022.

[9] I. Szöke, M. Skácel, L. Mošner, J. Paliesek, and J. Černocký, "Building and evaluation of a real room impulse response dataset," *IEEE Journal of Selected Topics in Signal Processing*, vol. 13, no. 4, pp. 863–876, 2019.

[10] B. F. Katz, B. N. Postma, D. Poirier-Quinot, and J. Meyer, "Experience with a virtual reality auralization of Notre-Dame Cathedral," *The Journal of the Acoustical Society of America*, vol. 141, no. 5, pp. 3454–3454, 2017.

[11] B. F. G. Katz, D. Murphy, and A. Farina, "Exploring cultural heritage through acoustic digital reconstructions," *Physics Today*, vol. 73, no. 12, pp. 32–37, 2020.

[12] G. Götz, R. Falcón Pérez, S. J. Schlecht, and V. Pulkki, "Neural network for multi-exponential sound energy decay analysis," *The Journal of the Acoustical Society of America*, vol. 152, no. 2, pp. 942–953, 2022.

[13] A. Ratnarajah, Z. Tang, R. Aralikatti, and D. Manocha, "Mesh2ir: Neural acoustic impulse response generator for complex 3d scenes," in *Proceedings of the 30th ACM International Conference on Multimedia*, MM '22, (New York, NY, USA), p. 924–933, Association for Computing Machinery, 2022.

[14] T. McKenzie, S. J. Schlecht, and V. Pulkki, "Acoustic analysis and dataset of transitions between coupled rooms," in *ICASSP 2021 - 2021 IEEE International Conference on Acoustics, Speech and Signal Processing (ICASSP)*, pp. 481–485, 2021.

[15] C. Schissler, P. Stirling, and R. Mehra, "Efficient construction of the spatial room impulse response," in *Proc. IEEE Virtual Reality*, pp. 122–130, Apr. 2017.

[16] L. Mccormack, A. Politis, T. Mckenzie, C. Hold, and V. Pulkki, "Object-based six-degrees-of-freedom rendering of sound scenes captured with multiple ambisonic receivers," *J. Audio Eng. Soc.*, vol. 70, pp. 355–372, may 2022.

[17] A. Neidhardt, C. Schneiderwind, and F. Klein, "Perceptual matching of room acoustics for auditory augmented reality in small rooms - literature review and theoretical framework," *Trends in Hearing*, vol. 26, 2022.

[18] S. Amengual Garí, P. Robinson, and P. Calamia, "Room acoustic characterization for binaural rendering: From spatial room impulse responses to deep learning," in *Proc. Int. Conf. on Acoustics (ICA)*, (Gyeongju, Korea), 10 2022.

[19] T. Deppisch, S. V. A. Garí, P. Calamia, and J. Ahrens, "Direct and residual subspace decomposition of spatial room impulse responses," *IEEE/ACM Trans. Audio, Speech and Lang. Proc.*, vol. 31, p. 927–942, jan 2023.

[20] W. G. Gardner, "Efficient convolution without input-output delay," *J. Audio Eng. Soc.*, vol. 43, pp. 127–136, Nov. 1995.

[21] L. McCormack, V. Pulkki, A. Politis, O. Scheuregger, and M. Marschall, "Higher-order spatial impulse response rendering: Investigating the perceived effects of spherical order, dedicated diffuse rendering, and frequency resolution," *J. Audio Eng. Soc.*, vol. 68, pp. 338–354, Jun. 2020.

[22] M. Berzborn and M. Vorländer, "Investigations on the directional energy decay curves in reverberation rooms," in *Proc. of Euronoise*, (Crete, Greece), May 2018.

[23] M. Nolan, E. Fernandez-Grande, J. Brunskog, and C.-H. Jeong, "A wavenumber approach to quantifying the isotropy of the sound field in reverberant spaces," *J. Acoust. Soc. Am.*, vol. 143, pp. 2514–2526, Apr. 2018.

[24] M. Nolan, M. Berzborn, and E. Fernandez-Grande, "Isotropy in decaying reverberant sound fields," *J. Acoust. Soc. Am.*, vol. 148, pp. 1077–1088, Aug. 2020.

[25] B. Alary, P. Massé, S. J. Schlecht, M. Noisternig, and V. Välimäki, "Perceptual analysis of directional late reverberation," *J. Acoust. Soc. Am.*, vol. 149, pp. 3189–3199, May 2021.

[26] B. Alary and V. Välimäki, "A method for capturing and reproducing directional reverberation in six degrees of freedom," in *Proc. Int. Conf. Immersive and 3D Audio*, (Bologna, Italy), Sep 2021.

[27] B. Alary, A. Politis, S. J. Schlecht, and V. Välimäki, "Directional feedback delay network," *J. Audio Eng. Soc.*, vol. 67, pp. 752–762, Oct. 2019.

[28] B. Alary and A. Politis, "Frequency-dependent directional feedback delay network," in *Proc. IEEE ICASSP-2020*, pp. 176–180, May 2020.

[29] International Organization for Standardization, *ISO 3382-1: 2009. Acoustics - Measurement of Room Acoustic Parameters*. Geneva, Switzerland: ISO, 2009.

[30] D. Griesinger, "Beyond mls-occupied hall measurement with fft techniques," in *Proc. Audio Eng. Soc. 101st Conv.*, (Los Angeles, USA), Nov. 1996.

[31] A. Farina, "Simultaneous measurement of impulse response and distortion with a swept-sine technique," in *Proc. Audio Eng. Soc. 108th Conv.*, Feb. 2000.

[32] M. R. Schroeder, "New method of measuring reverberation time," *J. Acoust. Soc. Am.*, vol. 37, pp. 409–412, Mar. 1965.

[33] J.-M. Jot, "An analysis/synthesis approach to real-time artificial reverberation," in *Proc. IEEE ICASSP-92*, vol. 2, (San Francisco, CA), pp. 221–224, Mar. 1992.

[34] P. Massé, T. Carpentier, O. Warusfel, and M. Noisternig, "Denoising directional room impulse responses with spatially anisotropic late reverberation tails," *Appl. Sci.*, vol. 10, p. 1033, Feb. 2020.

[35] N. Epain and C. T. Jin, "Spherical harmonic signal covariance and sound field diffuseness," *CoRR*, vol. abs/1607.00211, Jul. 2016.